Figure S1

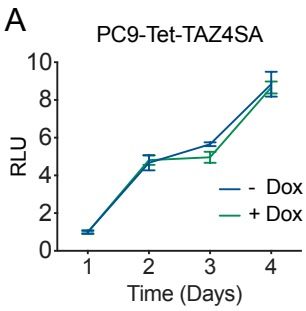

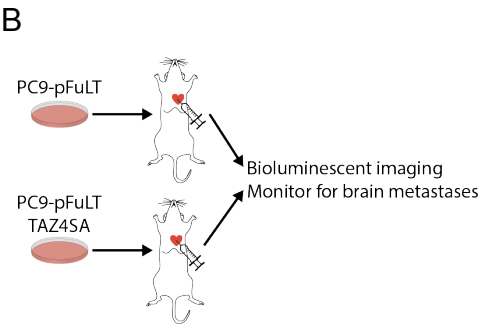

C

Cell Line	Brain metastasis	*p*-value (χ^2)	Median BMFS (days)
PC9-pFuLT	4/13 (31%)	0.0123	Undefined*
PC9-pFuLT-TAZ4SA	13/17 (76%)		22
PC9-BrM3 shNTC	8/10 (80%)	0.0246	30.5
PC9-BrM3 shTAZ	3/10 (30%)		Undefined*

*denotes group did not reach median survival (50%) by end of study

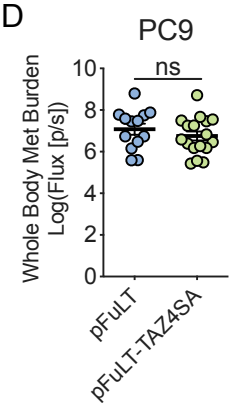

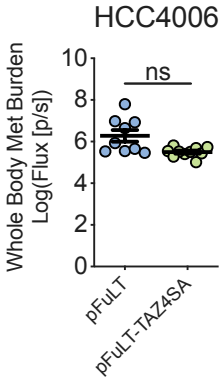

F

GSEA - Hallmark Signature Set

Signature	NES	NOM p-val
TAZ4SA	**2.48**	**<0.001**
EMT	2.44	<0.001
HYPOXIA	2.30	<0.001
APICAL JUNCTION	2.14	<0.001
TGF BETA SIGNALING	2.03	<0.001
MYOGENESIS	1.94	<0.001
UV RESPONSE DN	1.94	<0.001
CHOLESTEROL HOMEOSTASIS	1.93	<0.001
COAGULATION	1.79	<0.001

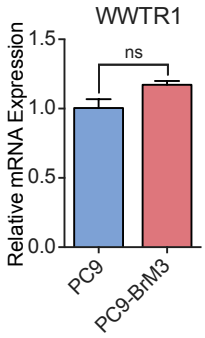

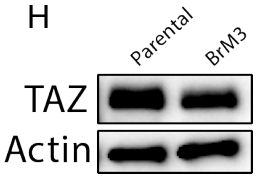

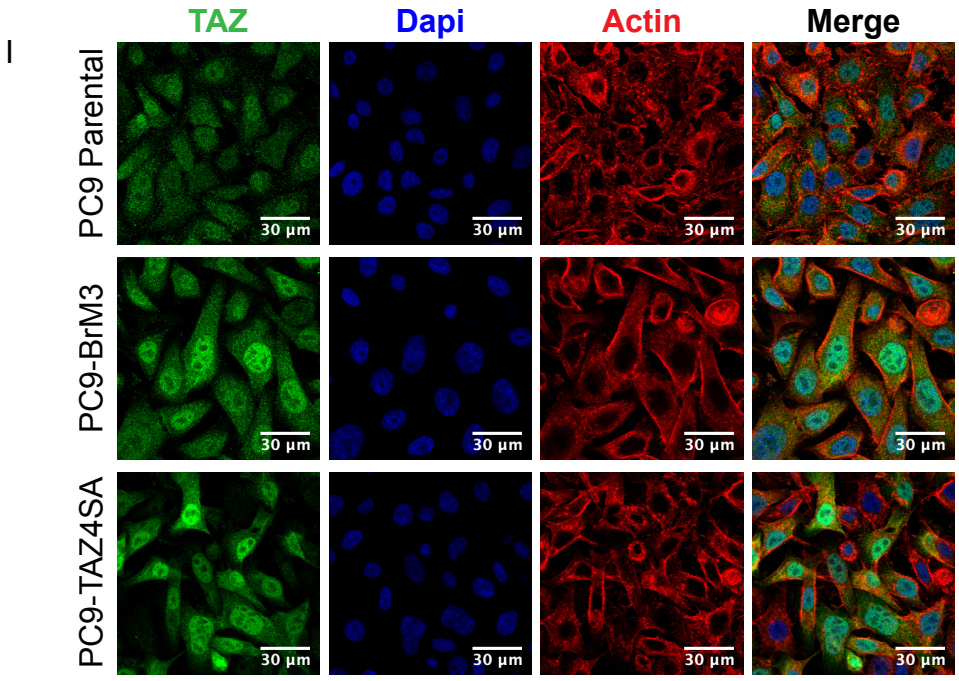

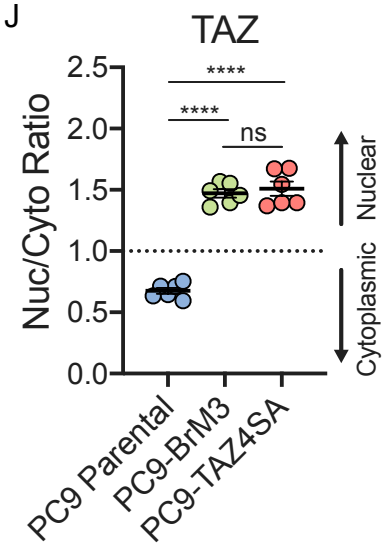

Supplemental Figure S1. Active TAZ promotes brain metastasis and TAZ nuclear accumulation is enhanced in brain metastatic lung adenocarcinoma cells. Related to Figure 1. A) Cell-Titer Glo assay measuring cell viability of PC9-Tet-TAZ4SA cells treated +/- dox in 2D culture (n=5). Error bars represent the mean +/- SEM. **B)** Schematic of study design to measure brain metastasis in pFuLT parental vs pFuLT-Tet-TAZ4SA-expressing lung cancer cells. **C)** Table comparing percentages of brain metastasis-bearing mice between experimental groups; p-values calculated by Chi-square test. **D-E)** Quantification of whole-body metastatic burden in mice injected with **D)** PC9-pFuLT (n=13) vs PC9-pFuLT-Tet-TAZ4SA (n=17) cells or **E)** HCC4006-pFuLT (n=9) vs HCC4006-pFuLT-Tet-TAZ4SA (n=10) cells. **F)** Table of TAZ4SA gene signature and other top PC9-BrM3-enriched signatures of the Hallmark signature gene set from mSigDB. **G)** RT-qPCR of *WWTR1* mRNA (n=3) and **H)** immunoblot analysis of TAZ protein in PC9 parental vs PC9-BrM3 cells. **I)** Representative immunofluorescence images and **J)** quantification of TAZ nuclear/cytoplasmic ratio in the indicated cell lines. TAZ4SA was used as positive control for nuclear TAZ. Statistical analysis conducted by one-way ANOVA followed by Fisher post-hoc testing (n=6); **** indicates p-value < 0.0001, ns=non-significant. Error bars represent the mean +/- SEM.

Figure S2

A

Gene Symbol	Log2 Fold Change
AXL	3.21
FGFR2	3.07
CSF1R	2.06
FYN	1.73
EPHA4	1.72
EPHB6	1.57
JAK3	0.95
MET	0.94
IGF1R	0.91
PTK2B	0.87
FGFR4	0.77
EPHB2	0.70
JAK1	0.70
EGFR	0.57
ROR1	0.57
ERBB2	0.48
SRC	0.47
TNK2	0.41
YES1	0.36
ABL2	0.35
EPHB4	0.33
PTK7	0.32
EPHA2	0.27

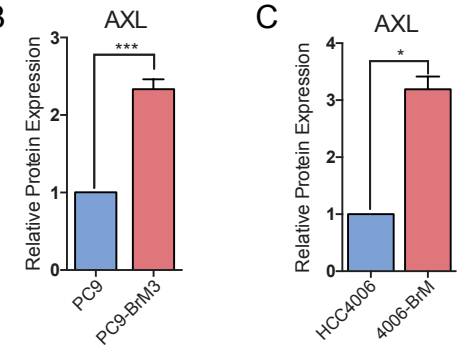

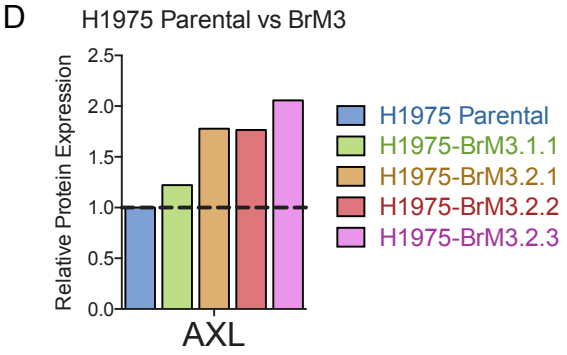

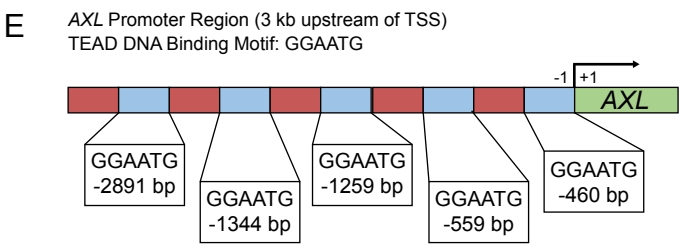

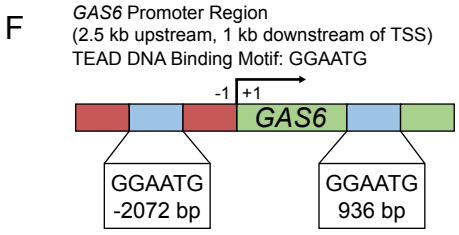

Supplemental Figure S2. Expression of the AXL receptor tyrosine kinase is upregulated in brain-metastatic lung cancer cells. Related to Figure 2. A) Table depicting top 23 kinases whose mRNA expression is upregulated in PC9-BrM3 cells. **B-C)** Quantification of AXL protein expression in **B)** PC9 parental vs PC9-BrM3 (n=3) or **C)** HCC4006 parental vs HCC4006-BrM cells (n=3). Data corresponds to representative immunoblots shown in main Figure 2E. **D)** Relative protein expression of AXL in H1975 parental and H1975-BrM3 cell lines derived from independent mice. Protein expression normalized to actin loading control. **E)** Diagram depicting TEAD DNA binding motifs upstream of the *AXL* transcriptional start site (TSS). **F)** Diagram depicting TEAD DNA binding motifs nearest the *GAS6* TSS; * p-value < 0.05, *** p-value < 0.001. Error bars represent the mean +/- SEM.

Figure S3

Prediction Algorithm/Model	ABL001	GNF-5	R428	TP-0903	Paclitaxel	Docetaxel
AdaBoost_MACCSFP BBB Score (>0 is BBB+)	4.196	3.296	3.941	1.109	-5.055	-4.466
AdaBoost_OpenbabelFP2 BBB Score (>0 is BBB+)	8.366	12.66	24.351	7.282	-9.163	-8.039
AdaBoost_Molprint2DFP BBB Score (>0 is BBB+)	5.122	4.491	5.946	-173.76	-0.497	-0.497
AdaBoost_PubChemFP BBB Score (>0 is BBB+)	13.64	16.63	14.52	9.66	-12.445	-8.266
SVM_MACCSFP BBB Score (>0.02 is BBB+)	0.024	0.06	0.051	0.032	-0.234	-0.213
SVM_OpenbabelFP2 BBB Score (>0 is BBB+)	0.066	0.15	-0.066	0.187	-0.188	-0.206
SVM_Molprint2DFP BBB Score (>0 is BBB+)	0.414	0.453	0.348	0.681	0.333	0.403
SVM_PubChemFP BBB Score (>0 is BBB+)	0.081	0.086	0.087	0.144	-0.528	-0.522

Supplemental Figure S3. Computational modeling predicts small molecule inhibitors of the ABL and AXL protein tyrosine kinases are blood-brain barrier penetrant. Related to Figure 6. Blood-brain barrier (BBB) permeability prediction algorithm scores for indicated small molecule inhibitors against the ABL kinases (ABL001 and GNF-5), or AXL (R428, also known as BGB324, and TP-0903). Paclitaxel and Docetaxel included as negative controls (non-BBB penetrant). CBLigand database was used for prediction modeling (https://www.cbligand.org/BBB/).

Figure S4

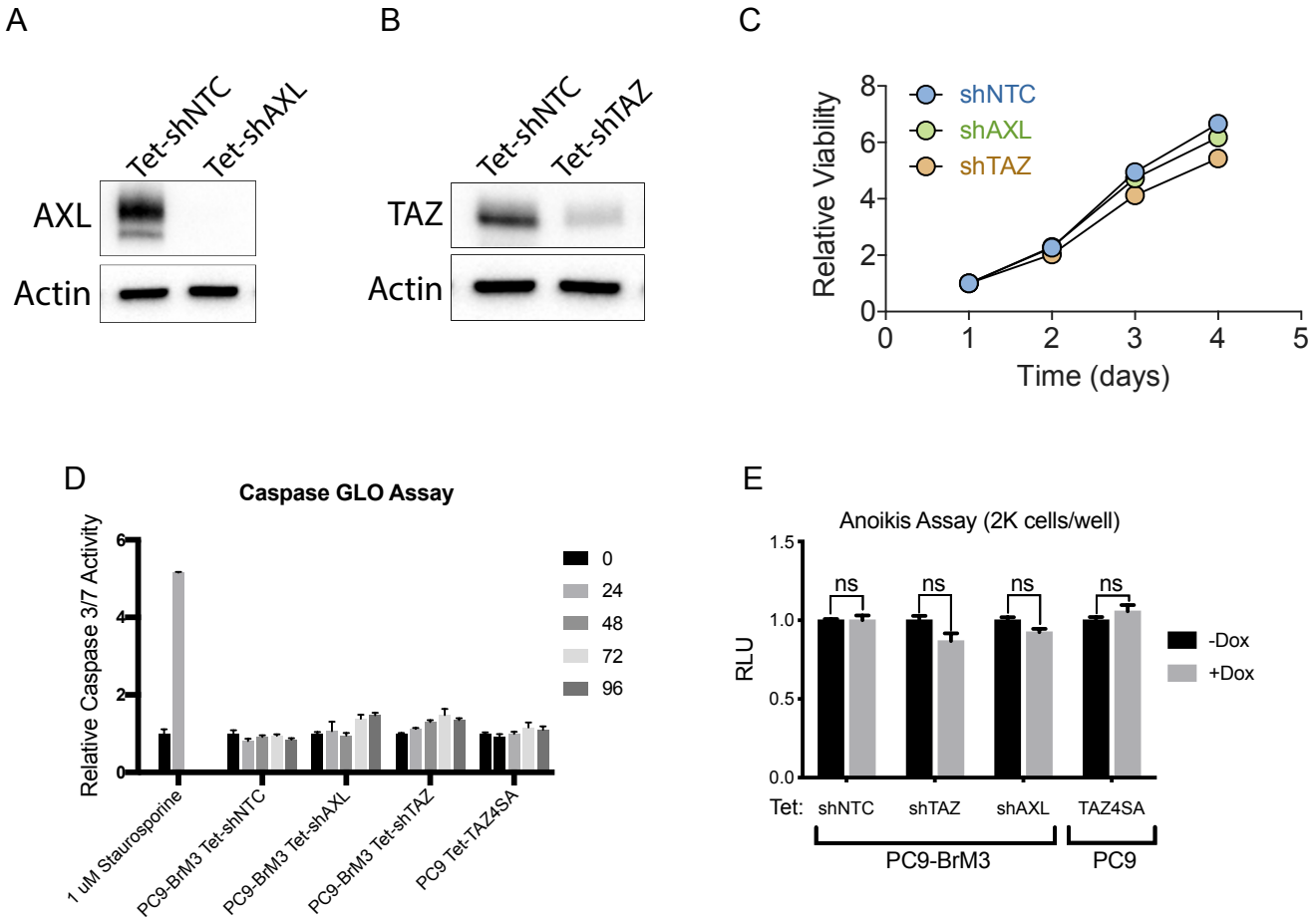

Supplemental Figure S4. Depletion of AXL and TAZ signaling does not influence cell proliferation, apoptosis, or anoikis of brain-metastatic lung cancer cells. Related to Figure 6. A) Immunoblots of the indicated proteins in PC9-BrM3 cells transduced with dox-inducible shNTC or shAXL and treated with 500 ng/mL dox for 72 h. **B)** Immunoblots of PC9-BrM3 cells transduced with dox-inducible sh-shNTC or shTAZ and treated with 500 ng/mL dox for 72 h. **C)** CellTiter GLO assay measuring cell viability in PC9-BrM3 cells transduced with stable shNTC, shAXL, or shTAZ; n=8 technical replicates. **D)** Caspase-GLO assay measuring relative Caspase 3/7 activity in PC9-BrM3 cells transduced with the indicated dox-inducible lentiviral shRNAs or PC9 parental cells lentivirally transduced with Tet-TAZ4SA expression vector. Cells transduced with inducible constructs were treated with 500 ng/mL dox for the indicated timepoints (in hours). Dox and fresh media were replaced every 24 h prior to assay. PC9-BrM3 cells treated with 1 uM staurosporine for 24 h were used as a positive control. Error bars represent mean +/- SEM from two independent experiments. **E)** Anoikis assay in PC9-BrM3 cells transduced with the indicated dox-inducible lentiviral shRNAs or PC9 parental cells lentivirally transduced with Tet-TAZ4SA expression vector. Cells transduced with inducible constructs were seeded in ultra-low attachment 96-well plates and were treated with or without 500 ng/mL dox for 72 h. RLU=relative luminescent units. Statistical analysis performed by one-way ANOVA with Tukey post-hoc testing (n=5); ns = not significant.

Figure S5

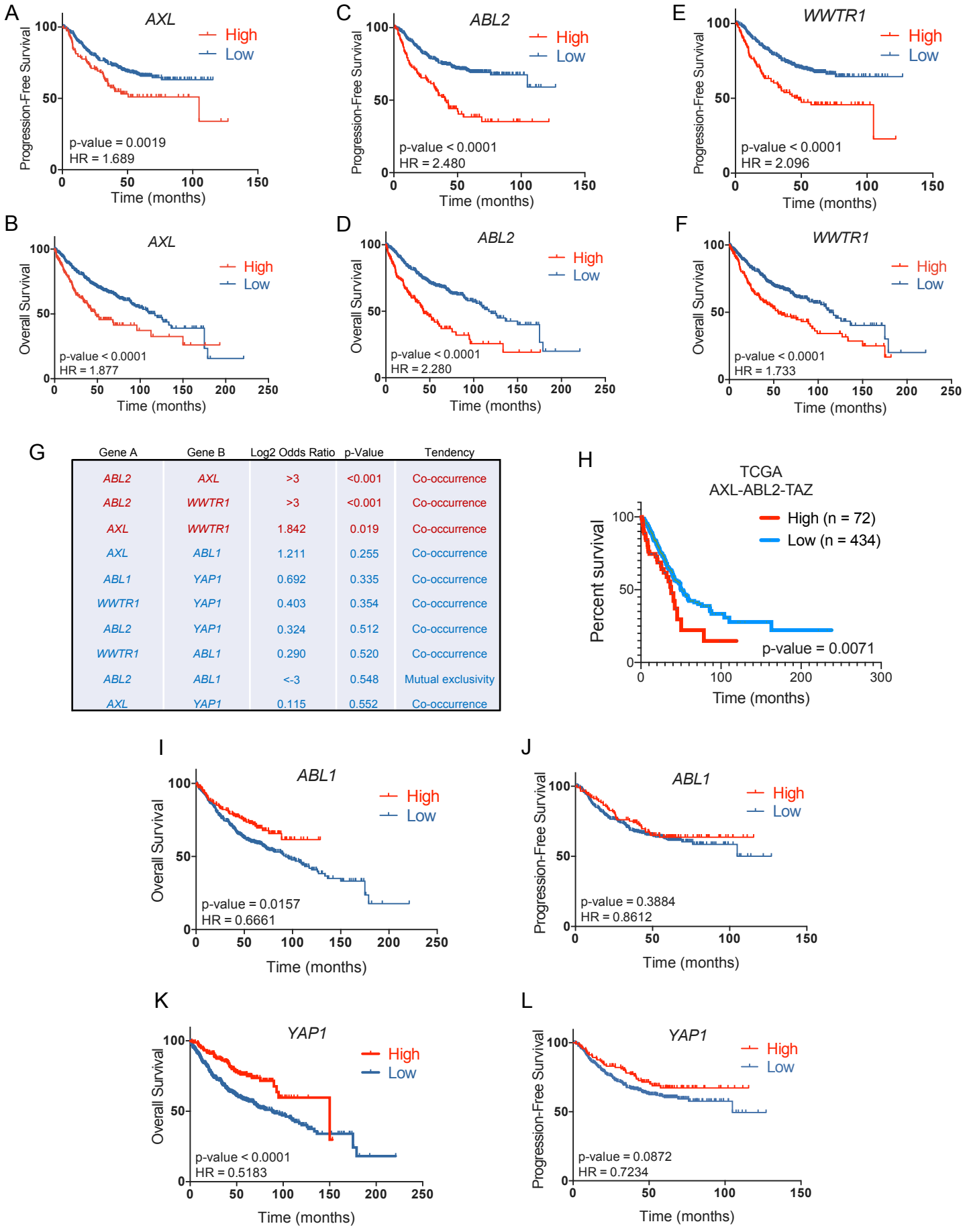

Gene A	Gene B	Log2 Odds Ratio	p-Value	Tendency
ABL2	*AXL*	>3	<0.001	Co-occurrence
ABL2	*WWTR1*	>3	<0.001	Co-occurrence
AXL	*WWTR1*	1.842	0.019	Co-occurrence
AXL	*ABL1*	1.211	0.255	Co-occurrence
ABL1	*YAP1*	0.692	0.335	Co-occurrence
WWTR1	*YAP1*	0.403	0.354	Co-occurrence
ABL2	*YAP1*	0.324	0.512	Co-occurrence
WWTR1	*ABL1*	0.290	0.520	Co-occurrence
ABL2	*ABL1*	<-3	0.548	Mutual exclusivity
AXL	*YAP1*	0.115	0.552	Co-occurrence

Supplemental Figure S5. High expression of *ABL2, AXL,* and *WWTR1,* but not *ABL1* or *YAP1,* correlates with poor survival outcomes in human lung adenocarcinoma patients. Related to Figure 6. A-F) OS and progression-free survival (PFS) curves derived from human lung adenocarcinoma patient microarray datasets with high versus low expression of *AXL* **(A-B)**, *ABL2* **(C-D)** or *WWTR1* **(E-F)**. Curves were generated using KMPlot analysis tool. For OS, patients were stratified into high (upper quartile, *n* = 180 patients) vs low (bottom three quartiles, *n* = 540 patients) expression for the indicated genes. For PFS, patients were stratified into high (upper quartile, *n* = 114 patients) vs low (bottom three quartiles, *n* = 347 patients) expression. **G)** Mutual exclusivity analysis of *AXL*, *ABL1*, *ABL2*, *WWTR1*, and *YAP1* combined mRNA and protein expression in lung adenocarcinoma patients from the TCGA Provisional dataset. Data analyzed using the cBioPortal online analysis software. **H)** Kaplan-Meier analysis of OS in TCGA patient dataset for lung adenocarcinoma patients with high expression of AXL, ABL2 and TAZ. **I-L)** OS or PFS in lung adenocarcinoma patients stratified by high vs. low mRNA expression of *ABL1* **(I-J)** or *YAP1* **(K-L)** using KMPlot analysis tool. Patients were stratified into high (upper quartile, *n* = 180 patients) vs low (bottom three quartiles, *n* = 540 patients) expression for the indicated genes. For PFS curves, patients were also stratified into high (upper quartile, *n* = 114 patients) vs low (bottom three quartiles, *n* = 347 patients) expression. For all survival curves, statistical analysis performed by Log-rank (Mantel-Cox) test.

Figure S6

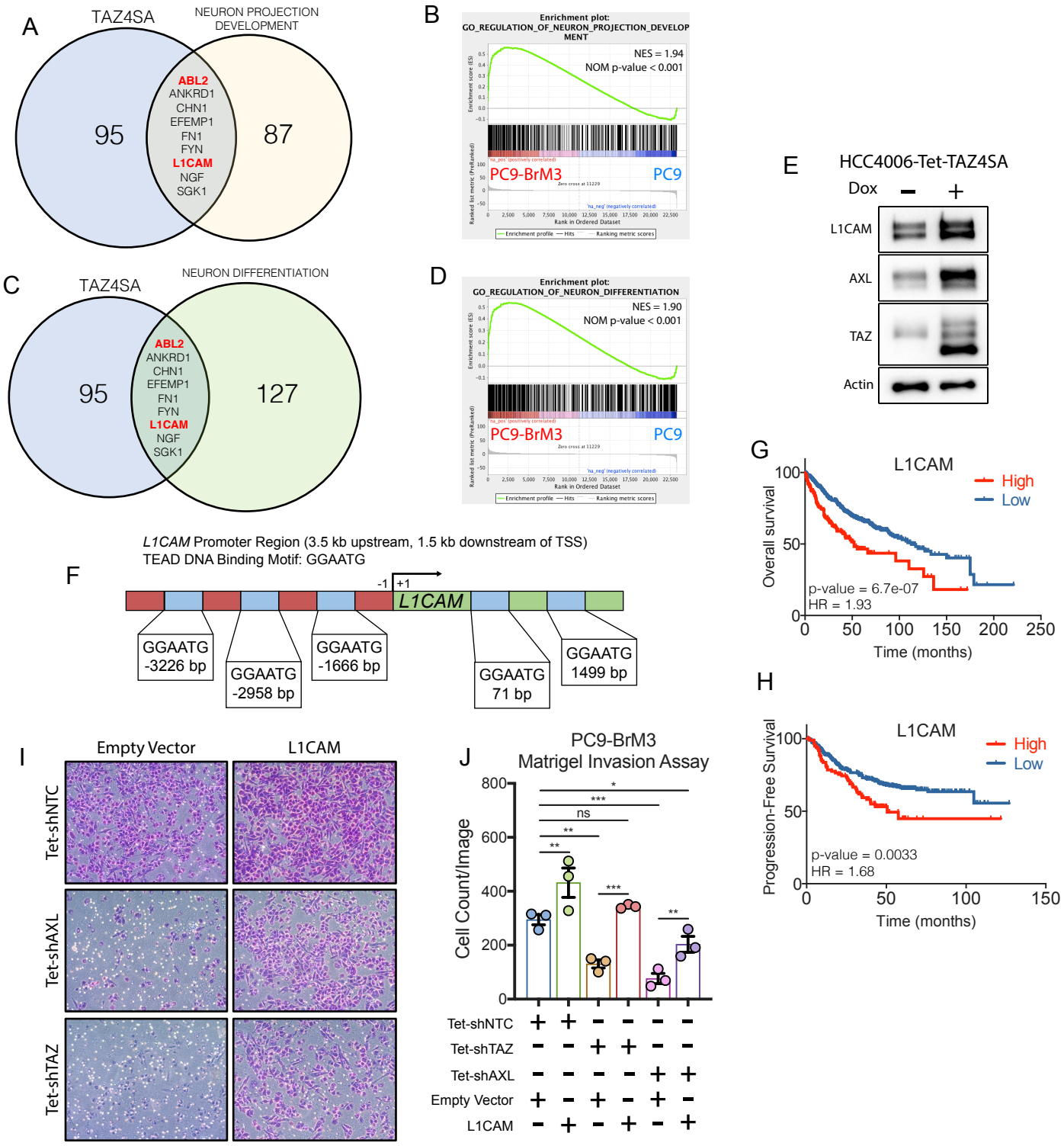

Supplemental Figure S6. Comparative analysis of gene expression data reveals TAZ-dependent expression of neuronal signatures including *L1CAM* which drives a pro-invasive phenotype in brain-metastatic lung cancer cells. Related to Figure 7. A-D) Venn diagrams and corresponding GSEA plots of overlapping transcripts upregulated in the TAZ4SA GSEA signature and signatures for **A-B)** neuron projection development and **C-D)** neuron differentiation. Signatures were gathered from the Gene Ontology signature set available through mSigDB (The Broad Institute). **E)** Immunoblots of HCC4006-Tet-TAZ4SA cells treated with or without 500 ng/mL dox for 5 days. **F)** Diagram depicting TEAD DNA binding motifs in proximal and distal sequences of the *L1CAM* TSS. **G-H)** Kaplan-Meier analysis of **H)** OS (high $n = 172$, low $n = 548$) and **I)** PFS (high $n = 100$, low $n = 361$) in patients with high vs low mRNA expression of *L1CAM*. Statistical analysis performed by Log-rank (Mantel-Cox) test. **I)** Representative images and **J)** quantification of matrigel invasion assay in PC9-BrM3 cells transduced with dox-inducible shNTC, shAXL, or shTAZ as well as stable expression through lentiviral transduction of empty vector control or *L1CAM* cDNA. Cells from eight non-overlapping images per condition from three independent experiments were counted and the means from each condition were graphed. Statistical analysis performed by one-way ANOVA with Fisher post-hoc testing. Error bars represent mean +/- SEM. ns = non-significant, * p-value < 0.05, ** p-value < 0.01, *** p-value < 0.005.

Supplemental Table S1. Gene List for TAZ4SA Signature. Related to Figure 1.

F3	SGK1	RELB	GLIS3	PSG1
FN1	FSTL3	FA2H	ANKRD2	IL6
THBS1	EEF1A2	HLA-B	C4orf19	APLN
IGFBP3	LATS2	CSRNP1	DYRK3	CYP4V2
PTRF	HEG1	PLCXD2	LANCL3	VANGL2
WWTR1	MAOA	CCRN4L	EFEMP1	SCG2
CYR61	RBMS2	BMP4	ADAMTS6	TAGLN
CRIM1	C1orf116	ATF3	TMEM52B	DUSP8
EXT1	NFKB2	SFTA1P	HES7	SERTAD4-AS1
AXL	LIFR	CORO6	SLC7A7	TMCC2
EPB41L2	RN7SL1	ZNF462	ECM1	TRPM2
PLK2	DUSP1	MOB3B	HECTD2	SAA1
TNIP1	BIRC3	ARHGAP22	SLFN12	MYCL
UGCG	ADM	PAPSS2	B4GALNT3	NAV3
ABL2	CR2	CHIC2	TLR2	MMP19
OLR1	TFPI2	CDH13	MCOLN3	PHACTR3
SAV1	CDKN1A	GNB4	SYNPO	C6orf15
ETS1	EGR1	HSD3B1	MFAP5	SLC16A10
ANKRD1	IGFN1	MATN3	COL4A4	HLA-F
MAP3K14	MITF	MAPRE2	STK33	RP11-173M1.8
GABARAPL1	L1CAM	RAB30	CNKSR2	LHX4
MARCH4	SNAI2	GADD45B	UST	CTGF
TUFT1	MFGE8	EDN1	OSBPL6	C4BPB
AMOTL2	SGPP2	TRIM17	ARL4D	HPCAL4
FYN	HDAC9	STYK1	AC002480.3	TCF7L1
GADD45A	CST6	DAB2	SYNGR3	PSG5
ICAM1	GPR176	TNFSF15	MIR503HG	AASS
SLC2A3	GAS6	NGF	MT-TT	RP11-248J18.2
FAM126A	MYBL1	IQCJ-SCHIP1	GLI2	VSTM1
MAPK8	FBXO32	TMEM40	LINC00707	IL32
CITED2	NUAK2	STOM	CHN1	TNFRSF9
GJC1	ARHGEF26	KRT34	CDK14	BTG2
SRGN	DNAJC6	HHAT	MT-TI	HCP5
PPP1R15A	TMEM45A	PAX9	SCML2	PLAGL1
SLC26A2	GLIS2	RP11-145M9.4	DYRK1B	KRTAP2-3
TNC	A4GALT	SH2D5	ZBED2	DUSP9
RN7SL2	OSR2	PRR5L	HTRA3	FLJ00418
CD55	COL5A1	AGPAT4	PTPRB	KRT4
SERTAD4	RAB3B	HSPB8	FGF1	RNF125
AJUBA	EMB	ST3GAL6	BRSK1	PSG9

Supplemental Table S2. List of primers and oligonucleotides. Related to Key Resources Table.

Primer (Application)	**Source**	**Oligo Sequence**
18S-F (RT-qPCR)	Sigma	GAGGATGAGGTGGAACGTGT
18S-R (RT-qPCR)	Sigma	AGAAGTGACGCAGCCCTCTA
AXL-F (RT-qPCR)	Sigma	GTGGGCAACCCAGGGAATATC
AXL-R (RT-qPCR)	Sigma	GTACTGTCCCGTGTCGGAAAG
ABL1-F (RT-qPCR)	Sigma	AAGCCGCTCGTTGGAACTC
ABL1-R (RT-qPCR)	Sigma	AGACCCGGAGCTTTTCACCT
ABL2-F (RT-qPCR)	Sigma	GTTGAACCCCAGGCACTAAAT
ABL2-R (RT-qPCR)	Sigma	CAACGAAGAGATTAGGGTCACTC
GAS6-F (RT-qPCR)	Sigma	GCAAAACCTGCCTGACCAGT
GAS6-R (RT-qPCR)	Sigma	TTCGTTGACATCTTTGTCGCA
L1CAM-F (RT-qPCR)	Sigma	TGTCATCACGGAACAGTCTCC
L1CAM-R (RT-qPCR)	Sigma	CTGGCAAAGCAGCGGTAGAT
WWTR1-F (RT-qPCR)	Sigma	GATCCTGCCGGAGTCTTTCTT
WWTR1-R (RT-qPCR)	Sigma	CACGTCGTAGGACTGCTGG
ABL2 ChIP-F	Sigma	GGCTGGGAGGGAGAGACC
ABL2 ChIP-R	Sigma	ATTGAAGCCGGTCTCTGTGG
UTR ChIP-F	Sigma	GAGAAACCACAGAGCACCCA
UTR ChIP-R	Sigma	GGCGCCCAGGGTGATTTTTA
TAZ Y321F FWD (mutagenesis)	Sigma	TTGTGGGGACACTGAAGCACCCTAACCCC
TAZ Y321F REV (mutagenesis)	Sigma	GGGGTTAGGTGCTTCAGTGTCCCCACAA
AXL Y779F FWD (mutagenesis)	Sigma	ACATCAAGGCAAACAGTCCATCCAGACAGTCC
AXL Y779F REV (mutagenesis)	Sigma	GGACTGTCTGGATGGACTGTTTGCCTTGATGTC
AXL Y821F FWD (mutagenesis)	Sigma	ATCCATGTTGACAAAGAGGATTTCGTCAGGCTCC
AXL Y821F REV (mutagenesis)	Sigma	GGAGCCTGACGAAATCCTCTTTGTCAACATGGAT
AXL Y830F FWD (mutagenesis)	Sigma	GGGGTTCAGGAAAACCTCCACCCTCATCC
AXL Y830F REV (mutagenesis)	Sigma	GGATGAGGGTGGAGGTTTTCCTGAACCCC
AXL Y866F FWD (mutagenesis)	Sigma	CATCCTGCTGGACGCTTTGTCCTCTGCC
AXL Y866F REV (mutagenesis)	Sigma	GGCAGAGGACAAAGCGTCCAGCAGGATG
ABL2 R198K FWD (mutagenesis)	Sigma	GCTGCTCTCACTCTCTTTGACCAGGAAGCTGCCG
ABL2 R198K REV (mutagenesis)	Sigma	GCGGCAGCTTCCTGGTCAAAGAGAGTGAGAGCAGC
ABL2 K317M FWD (mutagenesis)	Sigma	CTTCCTTCAGTGTCATCACAGCCACTGTAAGGCTGTACTT
ABL2 K317M REV (mutagenesis)	Sigma	AAGTACAGCCTTACAGTGGCTGTGATGACACTGAAGGAAG